Article

Cell Reports

Oncogenic BRAF-Mediated Melanoma Cell Invasion

Graphical Abstract

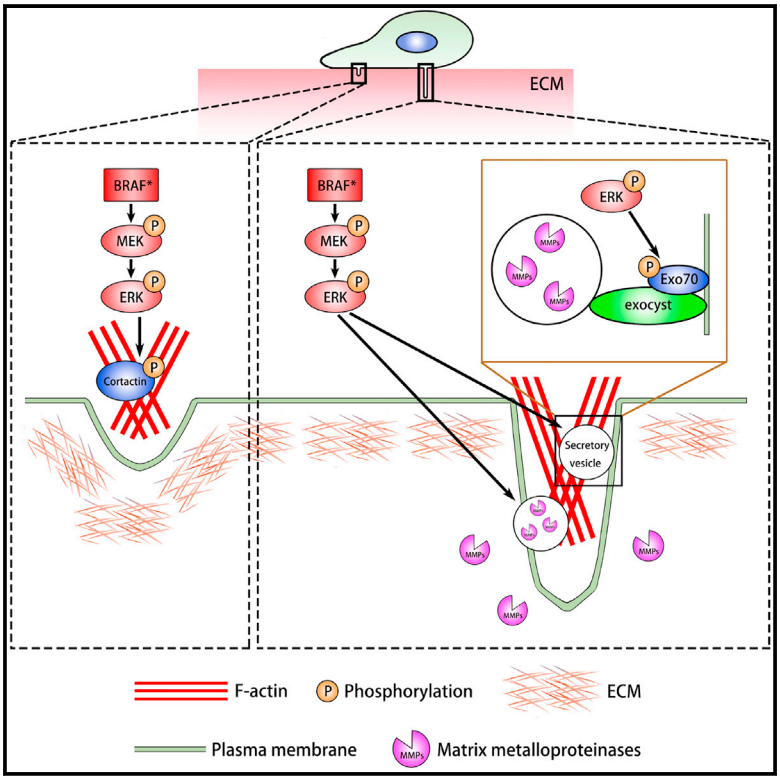

Highlights

- *BRAF*^{V600E} is involved in promoting melanoma cell invasion
- *BRAF*^{V600E} induces the phosphorylation of cortactin and Exo70 through ERK
- Inhibiting *BRAF*^{V600E} reduces invasion-related gene expression in a BRAF mouse model
- *BRAF*^{V600E} inhibition reduces cortactin foci formation in melanoma patient samples

Authors

Hezhe Lu, Shujing Liu, Gao Zhang, ..., Meenhard Herlyn, Xiaowei Xu, Wei Guo

Correspondence

xug@mail.med.upenn.edu (X.X.), guowei@sas.upenn.edu (W.G.)

In Brief

Lu et al. show that *BRAF*^{V600E} melanoma have extensive actin-based membrane protrusions and ECM degradation activity, which are mediated by ERK phosphorylation of cortactin and Exo70. The study implicates *BRAF*^{V600E} in melanoma invasion, in addition to its well-established role in tumorigenesis.

Lu et al., 2016, Cell Reports *15*, 2012–2024
May 31, 2016 © 2016 The Author(s).
http://dx.doi.org/10.1016/j.celrep.2016.04.073

OPEN ACCESS
CellPress

Cell Reports
Article

Oncogenic BRAF-Mediated Melanoma Cell Invasion

Hezhe Lu,[1,9] Shujing Liu,[2,9] Gao Zhang,[3] Lawrence N. Kwong,[4] Yueyao Zhu,[1] John P. Miller,[4] Yi Hu,[5] Wenqun Zhong,[1] Jingwen Zeng,[1] Lawrence Wu,[3] Clemens Krepler,[3] Katrin Sproesser,[3] Min Xiao,[3] Wei Xu,[6] Giorgos C. Karakousis,[7] Lynn M. Schuchter,[6] Jeffery Field,[8] Paul J. Zhang,[2] Meenhard Herlyn,[3] Xiaowei Xu,[2,*] and Wei Guo[1,*]

[1]Department of Biology, School of Arts and Sciences, University of Pennsylvania, Philadelphia, PA 19104, USA
[2]Department of Pathology and Laboratory Medicine, Perelman School of Medicine, University of Pennsylvania, Philadelphia, PA 19104, USA
[3]Molecular and Cellular Oncogenesis Program and Melanoma Research Center, The Wistar Institute, Philadelphia, PA 19104, USA
[4]Department of Translational Molecular Pathology, The University of Texas MD Anderson Cancer Center, Houston, TX 770303, USA
[5]Department of Biology, Drexel University, Philadelphia, PA 19104, USA
[6]Abramson Cancer Center and Department of Medicine, Perelman School of Medicine, University of Pennsylvania, Philadelphia, PA 19104, USA
[7]Department of Surgery, Hospital of the University of Pennsylvania, Philadelphia, PA 19104, USA
[8]Department of Systems Pharmacology and Translational Therapeutics, Perelman School of Medicine, University of Pennsylvania, Philadelphia, PA 19104, USA
[9]Co-first author
*Correspondence: xug@mail.med.upenn.edu (X.X.), guowei@sas.upenn.edu (W.G.)
http://dx.doi.org/10.1016/j.celrep.2016.04.073

SUMMARY

Melanoma patients with oncogenic *BRAF*^{V600E} mutation have poor prognoses. While the role of *BRAF*^{V600E} in tumorigenesis is well established, its involvement in metastasis that is clinically observed in melanoma patients remains a topic of debate. Here, we show that *BRAF*^{V600E} melanoma cells have extensive invasion activity as assayed by the generation of F-actin and cortactin foci that mediate membrane protrusion, and degradation of the extracellular matrix (ECM). Inhibition of *BRAF*^{V600E} blocks melanoma cell invasion. In a *BRAF*^{V600E}-driven murine melanoma model or in patients' tumor biopsies, cortactin foci decrease upon inhibitor treatment. In addition, genome-wide expression analysis shows that a number of invadopodia-related genes are downregulated after *BRAF*^{V600E} inhibition. Mechanistically, *BRAF*^{V600E} induces phosphorylation of cortactin and the exocyst subunit Exo70 through ERK, which regulates actin dynamics and matrix metalloprotease secretion, respectively. Our results provide support for the role of *BRAF*^{V600E} in metastasis and suggest that inhibiting invasion is a potential therapeutic strategy against melanoma.

INTRODUCTION

Malignant melanoma is well known for its aggressive metastasis, which accounts for most of patients' deaths (Erdmann et al., 2013). Approximately 50% of melanomas harbor activating mutations in the BRAF protein kinase. The most common BRAF mutation is the substitution of valine at position 600 by glutamic acid (V600E), which leads to constitutive activation of the kinase and thus the RAS-RAF-MEK-ERK pathway (Davies et al., 2002; Wan et al., 2004).

While the role of *BRAF*^{V600E} in driving melanomagenesis is well established, its role in melanoma invasion remains elusive, because conflicting evidence exists in the literature. In both cell culture and mouse models, oncogenic BRAF was reported to induce cancer cell invasion by activating the Rho family of guanosine triphosphatases (Makrodouli et al., 2011), downregulation of PDE5A (Arozarena et al., 2011), and reorganization of actin cytoskeleton (Klein et al., 2008). Studies also suggest that BRAF mutation alone does not induce metastasis and proteins such as β-catenin act as a central mediator of tumor metastasis in a *BRAF*^{V600E}/*PTEN*$^{-/-}$ mouse model of melanoma (Damsky et al., 2011). In clinical studies, the frequency of *BRAF*^{V600E} in metastatic melanomas is similar to primary melanomas (Casula et al., 2004; Colombino et al., 2012). In addition, BRAF or NRAS mutation status does not influence the clinical outcomes in patients with metastatic melanoma (Carlino et al., 2014). However, studies have shown that *BRAF*^{V600E} is correlated to a lower overall patient survival rate compared to BRAF wild-type melanoma, which is similar to what has been observed in other types of cancer (Cho et al., 2006; Davies et al., 2002; Long et al., 2011; Menzies et al., 2012; Nikiforova et al., 2003; Roth et al., 2010; Ugurel et al., 2007; Van Cutsem et al., 2011; Yokota et al., 2011). Clearly, a more definitive study of the role of *BRAF*^{V600E} in melanoma progression is needed.

Cancer cells initiate metastasis by invading through the extracellular matrix (ECM). To degrade the ECM, cells secrete metalloproteinases (MMPs) via actin-based membrane protrusions such as invadopodia (Hoshino et al., 2013b; Leong et al., 2014; Linder, 2007; McNiven, 2013; Murphy and Courtneidge, 2011; Paz et al., 2014; Yamaguchi, 2012). The formation of such invasion structures is controlled by signaling events that lead to phosphorylation of a number of proteins, including cortactin, which through neural Wiskott-Aldrich syndrome protein

This is an open access article under the CC BY license (http://creativecommons.org/licenses/by/4.0/).

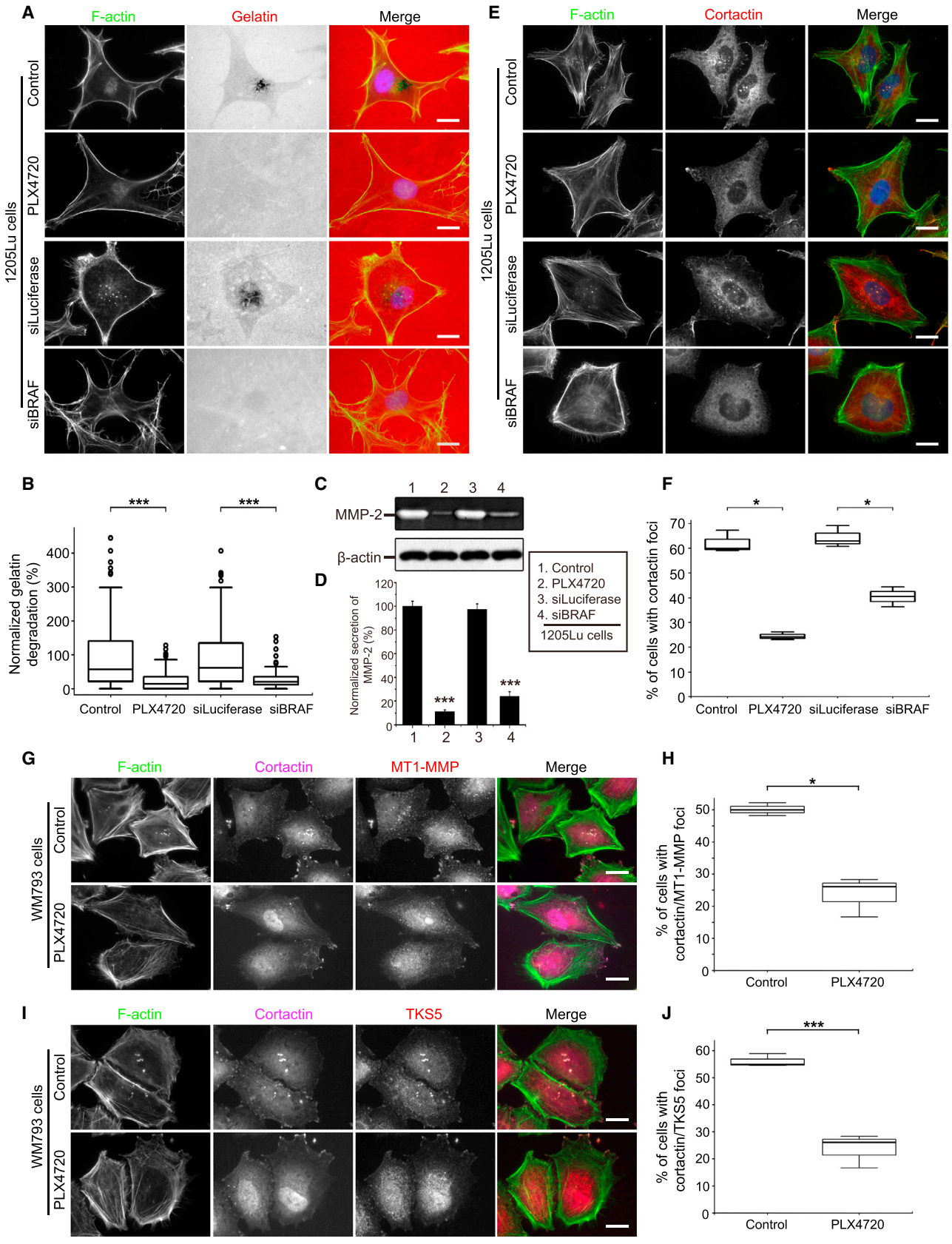

(legend on next page)

(N-WASP) and the Arp2/3 complex, initiates the dynamic reorganization of the F-actin network (Bravo-Cordero et al., 2012; Hoshino et al., 2013a, 2013b). Secretion of MMPs also requires the proper function of the exocytosis machinery. The exocyst, an octameric protein complex consisting of Sec3, Sec5, Sec6, Sec8, Sec10, Sec15, Exo70, and Exo84, mediates the docking of secretory vesicles to the plasma membrane during exocytosis (Wu and Guo, 2015; He and Guo, 2009; Hsu et al., 2004). Studies demonstrate that the exocyst is involved in MMP secretion and cell migration (Sakurai-Yageta et al., 2008; Liu et al., 2009; Lu et al., 2013; Ren and Guo, 2012; Monteiro et al., 2013). The exocyst subunit Exo70 is a direct phospho-substrate of ERK, which plays an important role in MMP secretion in response to growth factor signaling (Ren and Guo, 2012).

In this study, we systematically investigated the role of $BRAF^{V600E}$ in promoting melanoma invasion using a number of in vitro and in vivo approaches. We demonstrate that $BRAF^{V600E}$ is involved in melanoma cell invasion. Inhibition of $BRAF^{V600E}$ significantly reduces the number of cortactin foci in a genetically engineered, BRAF-driven mouse melanoma model and in melanoma patients' tumor biopsies. Mechanistically, $BRAF^{V600E}$ promotes ERK-dependent phosphorylation of both cortactin and Exo70, which in turn regulates actin assembly and MMP secretion. Genome-wide expression analysis shows a number of invadopodia-related genes are regulated by $BRAF^{V600E}$ expression. Taken together, our study suggests that $BRAF^{V600E}$ plays an important role in melanoma invasion.

RESULTS

$BRAF^{V600E}$ Is Necessary for Melanoma Cell Migration and Invasion

To investigate the role of $BRAF^{V600E}$ in controlling melanoma cell invasion, we first inhibited $BRAF^{V600E}$ with either small interfering RNA (siRNA) or the BRAF inhibitor PLX4720 in $BRAF^{V600E}$-positive melanoma cells. The WM3211 cell line with wild-type BRAF was included as a negative control. siRNA targeting both wild-type BRAF and $BRAF^{V600E}$ (siBRAF) (Poulikakos et al., 2011) effectively reduced the expression of BRAF in all four melanoma cell lines (Figures S1A and S1B). While siBRAF did not affect the motility of WM3211 cells with wild-type BRAF, the motility was significantly inhibited in $BRAF^{V600E}$-positive 1205Lu, WM35, and WM793 melanoma cell lines (Figure S1C). Similar to siBRAF, the BRAF inhibitor PLX4720 blocked the migration of 1205Lu, WM35, and WM793 cells (Figure S1D).

Next, we examined whether inhibition of $BRAF^{V600E}$ decreased the ability of melanoma cells to degrade ECM. The 1205Lu and WM793 cell lines treated with DMSO or transfected with control luciferase siRNA displayed a high level of gelatin degradation. In contrast, cells treated with PLX4720 or transfected with BRAF siRNA showed less degradation (Figures 1A and 1B; Figures S2A and S2B). MMP secretion mediates the degradation of the ECM (Murphy and Courtneidge, 2011). To test whether $BRAF^{V600E}$ regulates MMP secretion, we performed the zymography assay, which quantifies MMP activity by in-gel digestion of gelatin (Liu et al., 2008). The 1205Lu cells were transfected with siBRAF or treated with PLX4720. Conditioned media were collected and analyzed on a gel containing gelatin. As shown in Figures 1C and 1D, both PLX4720 and siBRAF significantly reduced the activity of MMP2 in the media.

Cancer cells invasion also requires actin-based membrane protrusions that penetrate into the ECM (Friedl and Wolf, 2003; Linder, 2007; Murphy and Courtneidge, 2011; Nürnberg et al., 2011). These invasion sites are often enriched with F-actin and its regulators, such as cortactin and Tks5, together with MMPs (Bowden et al., 1999; Eckert et al., 2011; Hoshino et al., 2013b; Sharma et al., 2013). Inhibition of $BRAF^{V600E}$ with either siBRAF or PLX4720 significantly reduced the number of F-actin/cortactin foci (Figures 1E and 1F; Figures S2C and S2D). The F-actin/cortactin foci were likely invadopodia, the actin-based membrane protrusions that penetrate into the ECM (Friedl and Wolf, 2003; Linder, 2007; Murphy and Courtneidge, 2011; Nürnberg et al., 2011). However, due to the fast actin dynamics and accumulative ECM degradation by MMPs, the F-actin/cortactin foci may not appear perfectly co-localized with the sites of ECM degradation. To further verify the invadopodia structures, we co-stained the cells for F-actin, cortactin, MT1-MMP, or Tks5. As shown in Figures 1G–1J and Figure S3, there were clear foci with co-localization of all three proteins in control cells, suggesting the formation of invadopodia. Upon PLX4720 treatment, the number of such foci was significantly decreased.

Figure 1. $BRAF^{V600E}$ Is Necessary for Actin-Based Membrane Protrusion Formation and ECM Degradation in Human $BRAF^{V600E}$ Melanoma Cells

(A) 1205Lu cells with different treatments were plated on coverslips coated with Alexa 568-labeled gelatin (red) for 12 hr. F-actin was stained with Alexa-488-phalloidin (green), and nuclei were stained with DAPI (blue). Areas of gelatin degradation were shown as black areas beneath the cells.

(B) Quantification of Alexa 568-labeled gelatin degradation. n > 150 from three independent experiments.

(C) In-gel zymography analysis shows that BRAF inhibition suppresses MMP-2 secretion in 1205Lu cells. The 1205Lu cells were transfected with siBRAF or treated with PLX4720 for 48 hr and then incubated with serum-free medium for 12 hr. Conditioned media were collected and analyzed on a gel containing gelatin.

(D) Quantification of MMP-2 secretion from different groups of cells in (C). n = 3.

(E) 1205Lu cells with different treatments were plated on coverslips coated with gelatin for 5 hr. Cells were stained with cortactin (red), phalloidin (green), and DAPI (blue).

(F) Quantification of the percentage of cells with cortactin foci. n > 150 from three independent experiments.

(G–J) WM793 cells with different treatments were plated on coverslips coated with gelatin for 5 hr (G and I). Cells were stained with cortactin (magenta), phalloidin (green), and MT1-MMP or TKS5 (red). Quantification of the percentage of cells with cortactin-MT1-MMP or cortactin-TKS5 foci (H and J). n > 150 from three independent experiments.

*p < 0.05, **p < 0.01, ***p < 0.001. Scale bars, 10 μm. Error bars, and SD. Kruskal-Wallis one-way ANOVA was performed in (B), (F), (H), and (J), and Student's t test was performed in (D) using software R v.2.14. See also Figures S1–S3.

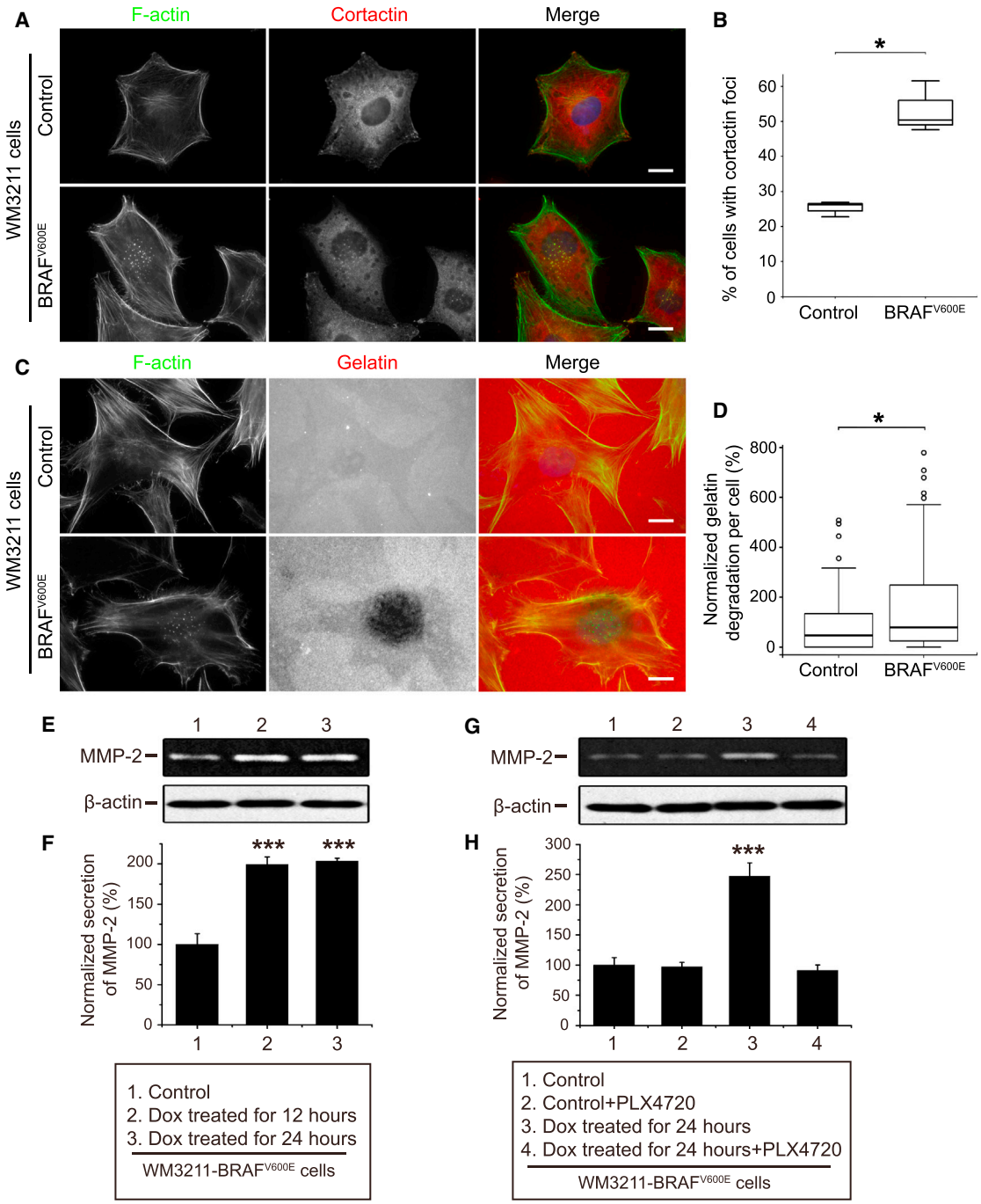

Figure 2. Transient Expression of *BRAF*^{V600E} Is Sufficient to Promote Melanoma Cell Invasion

(A) WM3211-*BRAF*^{V600E} cells were pretreated with Dox or DMSO for 4 hr and plated on coverslips coated with gelatin. The cells were still maintained in Dox except control. After 5 hr of incubation, cells were stained with cortactin (red), phalloidin (green), and DAPI (blue).

(B) Quantification of the percentage of cells with cortactin foci. n > 150 from three independent experiments.

(C) WM3211-*BRAF*^{V600E} cells were pretreated with Dox or DMSO for 4 hr and then plated on coverslips coated with Alexa 568-labeled gelatin (red). The cells were maintained in Dox except control. After 12 hr of incubation, cells were stained with F-actin (green) and nuclei (blue).

(D) Quantification of Alexa 568-labeled gelatin degradation. n > 150 from three independent experiments.

(E) In-gel zymography analysis shows the effect of *BRAF*^{V600E} on MMP-2 secretion in WM3211 cells. WM3211-*BRAF*^{V600E} cells were treated with or without Dox for indicated times, and the conditioned media were collected and analyzed by in-gel zymography. β-actin was detected by western blot.

(F) Quantification of MMP-2 secretion from different groups of cells in (E). n = 3.

(legend continued on next page)

Transient Expression of *BRAF*^{V600E} Is Sufficient to Induce Cell Invasion

To further validate the role of *BRAF*^{V600E} in melanoma cell invasion, we tested whether *BRAF*^{V600E} is sufficient to promote the formation of actin-based protrusion and ECM degradation. *BRAF*^{V600E} was expressed under the doxycycline (Dox)-inducible promoter in WM3211 cells that are wild-type for both BRAF and NRAS (henceforth termed WM3211-*BRAF*^{V600E} cells) (Figures S4A and S4B) (Meerbrey et al., 2011). After 9 hr of Dox treatment, the percentage of WM3211-*BRAF*^{V600E} cells with F-actin/cortactin foci was significantly higher than that of the WM3211 control cells (Figures 2A and 2B). Using fluorescence-labeled degradation assay, we further found that forced expression of *BRAF*^{V600E} increased gelatin degradation by approximately 1.5-fold compared to control cells (Figures 2C and 2D).

To test whether *BRAF*^{V600E} is sufficient to increase the secretion of MMPs, we measured MMP secretion in WM3211-*BRAF*^{V600E} cells with or without Dox treatment using an in-gel zymography assay. WM3211-*BRAF*^{V600E} cells displayed a more than 2-fold increase in MMP2 activity compared to that of the control cells (Figures 2E and 2F). To confirm that the increase in MMP2 activity was induced by *BRAF*^{V600E}, we treated cells with PLX4720 in the presence of Dox. PLX4720 significantly inhibited the MMP-2 activity that was induced by *BRAF*^{V600E} expression (Figures 2G and 2H). These data suggest that transient expression of *BRAF*^{V600E} is sufficient to promote ECM degradation.

We also found that expression of *BRAF*^{V600E} for 3 days induced cell growth arrest, and some cells exhibited the senescence-like phenotype (data not shown), similar to previous reports that *BRAF*^{V600E} induces cell growth arrest and senescence as a cellular response to oncogenic BRAF (Damsky et al., 2011, 2015; Dankort et al., 2009; Dhomen et al., 2009; Michaloglou et al., 2005; Vredeveld et al., 2012; Wajapeyee et al., 2008). This will be discussed further later.

BRAF^{V600E}-Mediated Invasion Is Dependent on ERK Phosphorylation of Cortactin and Exo70

Next, we set out to understand how *BRAF*^{V600E} promotes the assembly of protrusive actin structures and secretion of MMPs. Membrane protrusion is mediated by the recruitment and activation of actin regulatory proteins such as cortactin and Tks5 (Ayala et al., 2008; Seals et al., 2005). Cortactin can be phosphorylated at serine 418 (S^{418}) by ERK, which is a key kinase in the RAF-MEK-ERK cascade (Kelley et al., 2010; Martinez-Quiles et al., 2004). We therefore examined the phosphorylation of cortactin in response to *BRAF*^{V600E}. Forced expression of *BRAF*^{V600E} increased phospho-ERK levels and the phosphorylation of cortactin by ERK at S^{418} in WM3211-*BRAF*^{V600E} cells (Figure 3A). In addition, PLX4720 or siBRAF suppressed the phosphorylation of both ERK and cortactin in 1205Lu cells (Figure 3B). Furthermore, treatment of 1205Lu cells with two MEK inhibitors, U0126 or GSK1120212, significantly inhibited the phosphorylation of ERK and cortactin (Figures 3C and 3D). Fluorescence microscopy shows that these MEK inhibitors reduced the number of cells with cortactin foci by approximately 3-fold (Figures 3E–3H). Similarly, drug treatments significantly reduced the number of foci with co-localization of F-actin, cortactin, and Tks5 or those with co-localization of F-actin, cortactin, and MT1-MMP (Figures S5 and S6). These foci likely represent invadopodia.

Previous studies have shown that the exocyst mediates MMP secretion during invasion (Sakurai-Yageta et al., 2008; Liu et al., 2009; Monteiro et al., 2013; Ren and Guo, 2012). The exocyst subunit Exo70 coordinates actin dynamics with exocytosis to control cell invasion (Liu et al., 2009). ERK directly phosphorylates Exo70, thereby promoting exocytosis of MMPs (Ren and Guo, 2012). We therefore hypothesize that *BRAF*^{V600E} regulates MMP2 secretion through Exo70. To test this hypothesis, we determined whether Exo70 is required for MMP2 activity in *BRAF*^{V600E}-positive melanoma. Knockdown of Exo70 inhibited MMP2 secretion and gelatin degradation (Figures 4A–4C). Next, we examined the role of Exo70 in controlling tumor metastasis using a melanoma xenograft model. We generated 1205Lu stable cell lines expressing control short hairpin RNA (shRNA) or Exo70 shRNA (shExo70) and injected them into immunodeficient mice. Tumor metastasis was monitored over 5 weeks. While the incidence of primary tumor was similar for each group, knockdown of Exo70 effectively suppressed lung metastasis of 1205Lu cells (Figures 4D and 4E).

We performed an immunoprecipitation assay to determine the level of Exo70 phosphorylation. Phosphorylation of Exo70 increased more than 6-fold upon the forced expression of *BRAF*^{V600E} in WM3211 cells, while the total expression level of Exo70 remained unchanged (Figure 5A). We further examined whether *BRAF*^{V600E} promoted exocyst complex assembly, which is necessary for the tethering of secretory vesicles to the plasma membrane for exocytosis. As shown in Figures 5B and 5C, *BRAF*^{V600E} promoted the association of Exo70 with Sec8, another component of the exocyst complex. In addition, both PLX4720 and siBRAF suppressed Exo70 phosphorylation and its interaction with Sec8 (Figures 5D–5F). Because Exo70 is a substrate of ERK, we also examined the effect of inhibition of the BRAF-MEK-ERK pathway by a MEK inhibitor, U0126. As shown in Figures 5G–5I, after the treatment with U0126, phosphorylation of Exo70 decreased by approximately 6-fold, and the binding between Exo70 and Sec8 decreased by more than 5-fold.

BRAF^{V600E} Is Necessary for Invasion in a Genetically Engineered BRAF-Driven Mouse Melanoma

To further investigate the role of *BRAF*^{V600E} in vivo, we used a genetically engineered BRAF-driven mouse (iBIP mice, inducible

(G) In-gel zymography analysis shows that PLX4720 inhibits *BRAF*^{V600E}-induced MMP-2 secretion in WM3211 cells.
(H) Quantification of MMP-2 secretion from different groups of cells in (G). n = 3.
*$p < 0.05$, ***$p < 0.001$. Scale bars, 10 μm. Error bars, SD. Student's t test was performed in (F) and (H), and Kruskal-Wallis one-way ANOVA was conducted in (B) and (D) using software R v.2.14. See also Figure S4.

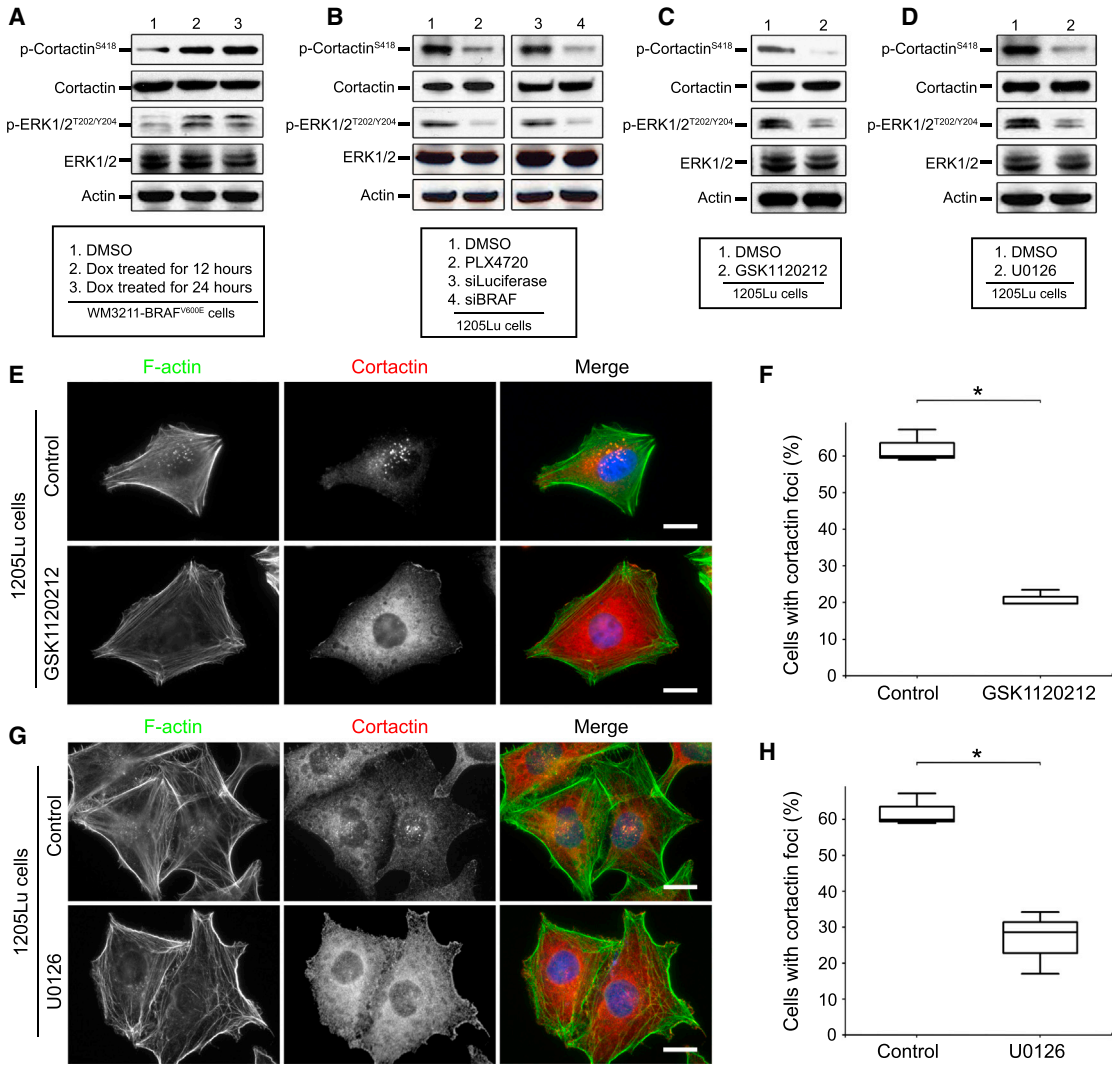

Figure 3. Actin-Based Membrane Protrusion Formation in *BRAF*^{V600E} Cells Is Dependent on ERK

(A) WM3211-*BRAF*^{V600E} cells were cultured with or without Dox for the indicated times and cell lysates were analyzed by western blot using antibodies against ERK1/2, phospho-ERK1/2 (p-ERK1/2), cortactin, phospho-cortactin (p-Cortactin^{S418}), and β-actin.

(B–D) Cell lysates from 1205Lu cells with different treatments were analyzed by western blot using antibodies against ERK1/2, p-ERK1/2, cortactin, p-Cortactin^{S418,} and β-actin.

(E–H) 1205Lu cells were treated with GSK1120212 or U0126 for 24 hr and then plated on coverslips coated with gelatin for 5 hr (E and G). Cells were stained with cortactin (red), phalloidin (green), and DAPI (blue). Quantification of the percentage of cells with cortactin foci. n > 150 from three independent experiments (F and H).

*p < 0.05. Scale bars, 10 μm. Kruskal-Wallis one-way ANOVA was performed using software R v.2.14. See also Figures S5 and S6.

BRAF INK/ARF PTEN) melanoma model (Kwong et al., 2015). As described previously, the iBIP mice were generated with a Tet-inducible human *BRAF*^{V600E} transgene on a melanocyte-specific, *Pten*-null, and constitutive *Cdkn2a*-null background. Mice with melanoma were treated with PLX4720 for 14 days. Pre-treatment and early-treatment biopsies from the same mouse were collected and stained with antibodies against cortactin (Eckert et al., 2011; Leong et al., 2014; Lu et al., 2013). While the pre-treatment tumor cells contained abundant cortactin foci, treating the mice with PLX4720 significantly reduced the number of cortactin foci (Figures 6A and 6B). During the time course of the experiment, no acquired BRAF inhibition (BRAFi) resistance was observed in the iBIP system.

To confirm the pharmacological effects and investigate the mechanism underlying *BRAF*^{V600E}-induced invasion, we took advantage of the Dox-controllable *BRAF*^{V600E} transgene. With extinction of *BRAF*^{V600E} expression upon Dox withdrawal, a longitudinal time course of 42 samples was analyzed by gene expression microarray (GEO: GSE79972). To understand the role of invadopodia regulation in relation to global gene expression, we first generated a knowledge-based invadopodia gene set consisting of 38 genes (Murphy and Courtneidge, 2011).

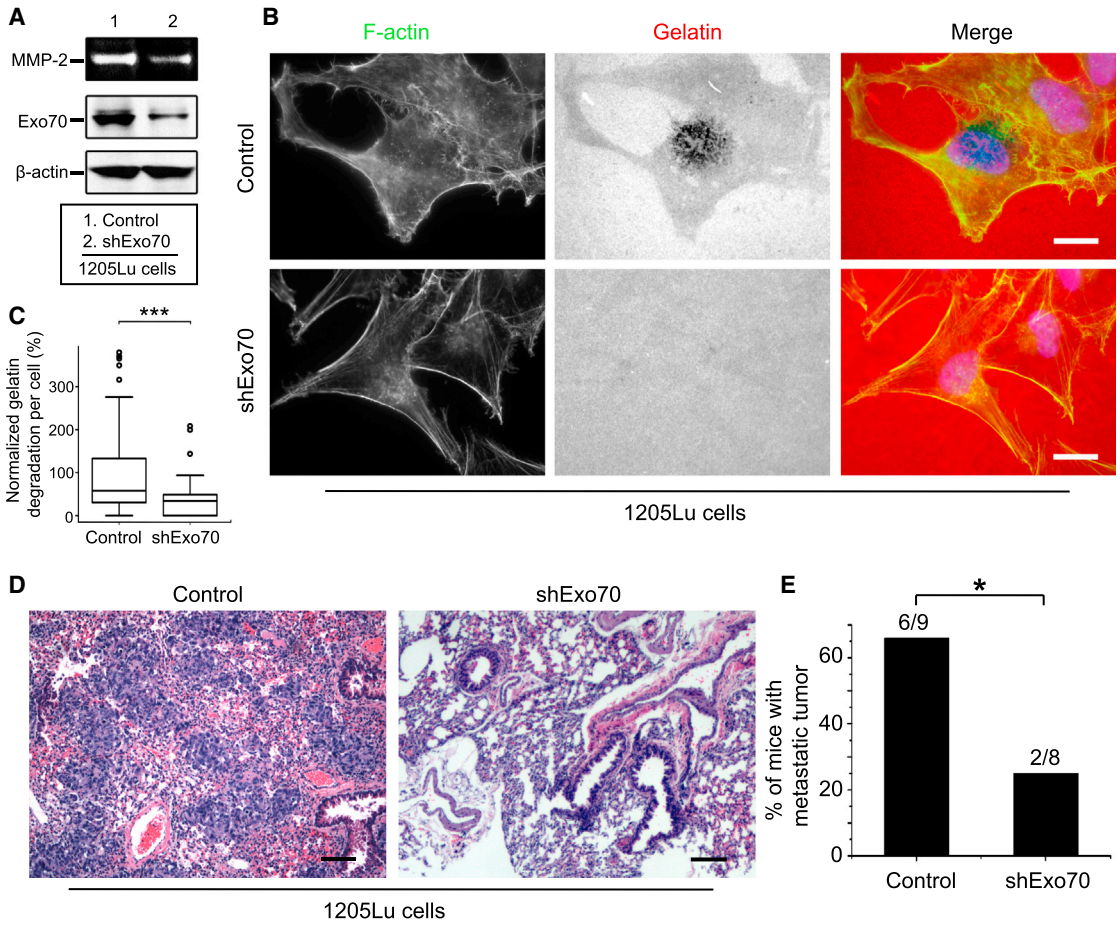

Figure 4. Exo70 Activity Is Required for the Gelatin Degradation and Melanoma Metastasis

(A) In-gel zymography analysis showed that Exo70 knockdown inhibited MMP-2 secretion in 1205Lu cells. Cell lysates from indicated cells were analyzed by western blot using anti-Exo70 and anti-β-actin antibodies.

(B) The gelatin degradation assay was performed in 1205Lu cells, which were transfected with Exo70 shRNA or vector control. Scale bars, 10 μm.

(C) Quantification of Alexa 568-labeled gelatin degradation per cell. n > 150 from three independent experiments.

(D) Representative images show H&E staining of metastatic tumor. Scale bars, 100 μm. The 1205Lu cells stably expressed vector control or Exo70 shRNA were injected into nude mice. Tissue samples were collected after 35 days.

(E) Percentage of mice with metastasis tumors among the two groups of mice.

*p < 0.05, ***p < 0.001. Error bars, SD. Student's t test was performed in (E), and Kruskal-Wallis one-way ANOVA was performed in (C) using software R v.2.14.

This includes regulatory kinases (e.g., RAC/RHO and PAKs), actin regulatory proteins (e.g., ARPC and WASL), and proteases (e.g., PLAUR and MMP9) that are implicated in different stages of invadopodia formation and function (Murphy and Courtneidge, 2011). Upon gene set enrichment analysis (GSEA) of genes that change over the full time course, we noted first that loss of BRAF activity resulted in significant downregulation of ERK signaling and of mitosis and cell-cycle-related gene sets (Figures 6C–6E). These expected results serve as positive controls that lend confidence to the analysis (Kwong et al., 2015). Strikingly, the invadopodia gene set is significantly downregulated, on par with cell-cycle genes, suggesting that invasion is one of the most prominent functions regulated by $BRAF^{V600E}$ in this model (Figures 6C–6E). Key genes including *RHOA*, *PAK1*, and *PAK3* are downregulated upon BRAF loss (Figure 6F), while others including *RAC1*, *CDC42*, and *CTTN* are downregulated at later time points. These are consistent with our PLX4720 IHC results. These microarray analyses suggest that oncogenic BRAF is essential for invadopodia formation in vivo and $BRAF^{V600E}$ inhibition modulates pathways that affect multiple stages of invasion.

Cortactin Foci in $BRAF^{V600E}$-Positive Melanoma Patients' Clinical Samples

To examine how oncogenic BRAF regulates invasion in human melanomas, we compared the cortactin foci in tumor biopsies derived from six BRAF-mutated, treatment-naive melanoma patients and those derived from seven wild-type BRAF treatment-naive melanoma patients. As shown in Figures 7A and 7B, the number of cortactin foci in $BRAF^{V600E}$ patients' tumor biopsies was significantly higher than that with wild-type BRAF. To determine whether BRAFi therapy decreased the number of cortactin

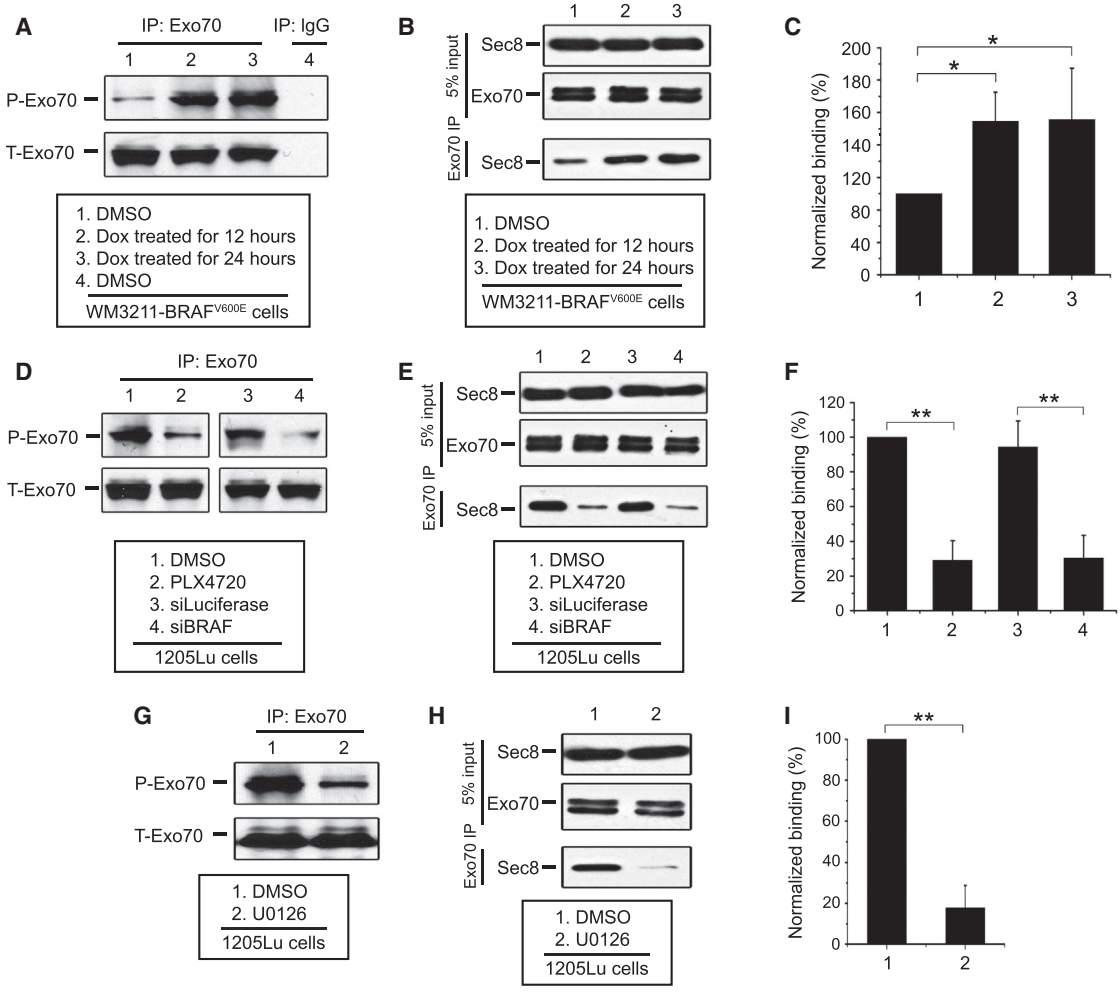

Figure 5. *BRAF*^{V600E} Promotes Exo70 Phosphorylation and Exocyst Complex Assembly

(A) Phosphorylation of endogenous Exo70. WM3211-*BRAF*^{V600E} cells were treated with or without Dox for the indicated times. Exo70 was immunoprecipitated from the cell lysates using the anti-Exo70 antibody. The immunoprecipitation protein complexes were analyzed by SDS-PAGE and probed for anti-ERK1/2 phospho-substrate antibody. The total levels of Exo70 were used as a loading control.

(B) WM3211-*BRAF*^{V600E} cells were treated with or without Dox for the indicated times, Exo70 and Sec8 were immunoprecipitated from the cell lysates and analyzed by SDS-PAGE and probed for Exo70 and Sec8.

(C) Quantification of Exo70 and Sec8 binding in (B).

(D) 1205Lu cells were treated with BRAF siRNA, luciferase siRNA, DMSO, or PLX4720. Exo70 was immunoprecipitated and analyzed as described in (A).

(E) 1205Lu cells were treated with BRAF siRNA, luciferase siRNA, DMSO, or PLX4720. Exo70 and Sec8 were immunoprecipitated from the cell lysates, analyzed by SDS-PAGE, and probed for Exo70 and Sec8.

(F) Quantification of Exo70 and Sec8 binding in (E).

(G) 1205Lu cells were treated with U0126, and Exo70 was immunoprecipitated and analyzed as described in (A).

(H) 1205Lu cells were treated with U0126. Exo70 and Sec8 were immunoprecipitated from the cell lysates, analyzed by SDS-PAGE, and probed for Exo70 and Sec8.

(I) Quantification of Exo70 and Sec8 binding in (H).

*$p < 0.05$, **$p < 0.01$. Error bars, SD. Student's t test was performed using software R v.2.14.

foci in vivo, we examined paired pre-treatment and early-treatment (2 weeks) tumor biopsies from three *BRAF*^{V600E}-positive patients treated with vemurafenib. Vemurafenib significantly inhibited cortactin foci formation as exhibited in all three melanoma patients' early-treatment tumor biopsies (Figures 7C and 7D). The data suggest a direct association between oncogenic BRAF and invasion in human melanomas.

DISCUSSION

Tumor cell invasion constitutes the initial stage of cancer metastasis. Here we studied the role of oncogenic BRAF in melanoma cell invasion. Our data suggest that oncogenic *BRAF*^{V600E} promotes melanoma cell invasion by stimulating the formation of actin structures and secretion of MMPs. Inhibiting *BRAF*^{V600E}

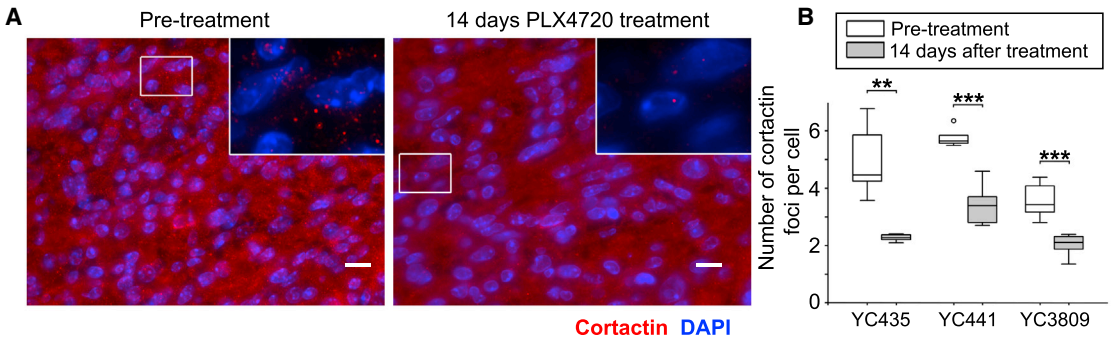

C

NAME	SIZE	NES	NOM p-val	FDR q-val
ERK SIGNALING	44	-3.09987	0	0
MITOSIS	67	-2.57891	0	0
REGULATION OF MITOSIS	34	-2.37027	0	0.002055
M PHASE OF MITOTIC CELL CYCLE	69	-2.35732	0	0.00203
MITOTIC CELL CYCLE	121	-2.32543	0	0.002035
INVADOPODIA RELATED GENE	38	-2.31599	0	0.002429
CELL CYCLE PROCESS	148	-2.26922	0	0.004806
M PHASE	84	-2.22725	0	0.007195
SPINDLE	36	-2.14337	0	0.015526

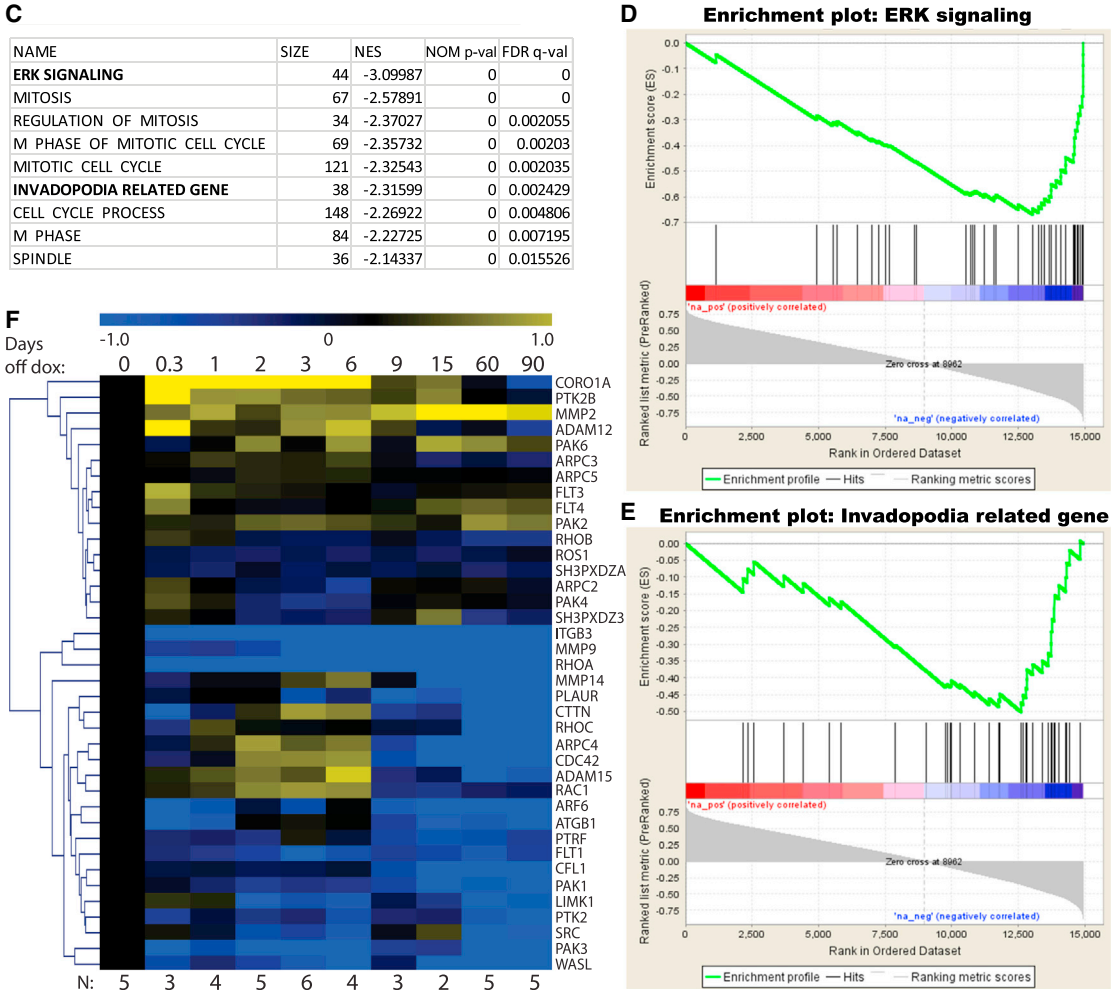

Figure 6. *BRAF*^{V600E} Is Necessary for Invasion in Genetically Engineered BRAF-Driven Mouse Melanoma Model

(A) Representative images of sections of iBIP mouse tumors stained with cortactin (red) and DAPI (blue). The sections are longitudinal biopsies from the same tumor pre- and post-BRAF inhibition by PLX4720.

(B) Quantification of cortactin foci in primary tumors. Three pairs of primary tumor biopsies from different mice were examined. Six field images were taken for each tumor sample.

(C–E) GSEA plots of the most significantly downregulated pathways after BRAF inhibition. Dox was withdrawn from iBIP mice to induce BRAF extinction in established tumors and then analyzed by expression microarray. Genes decreasing over a time course of 90 days were analyzed by GSEA.

(F) The heatmap of microarray data showing the expression levels of the invadopodia-related gene set in iBIP mice after genetic BRAF inhibition.

**p < 0.01, ***p < 0.001. Scale bars, 50 μm. Student's t tests were performed using software R v.2.14.

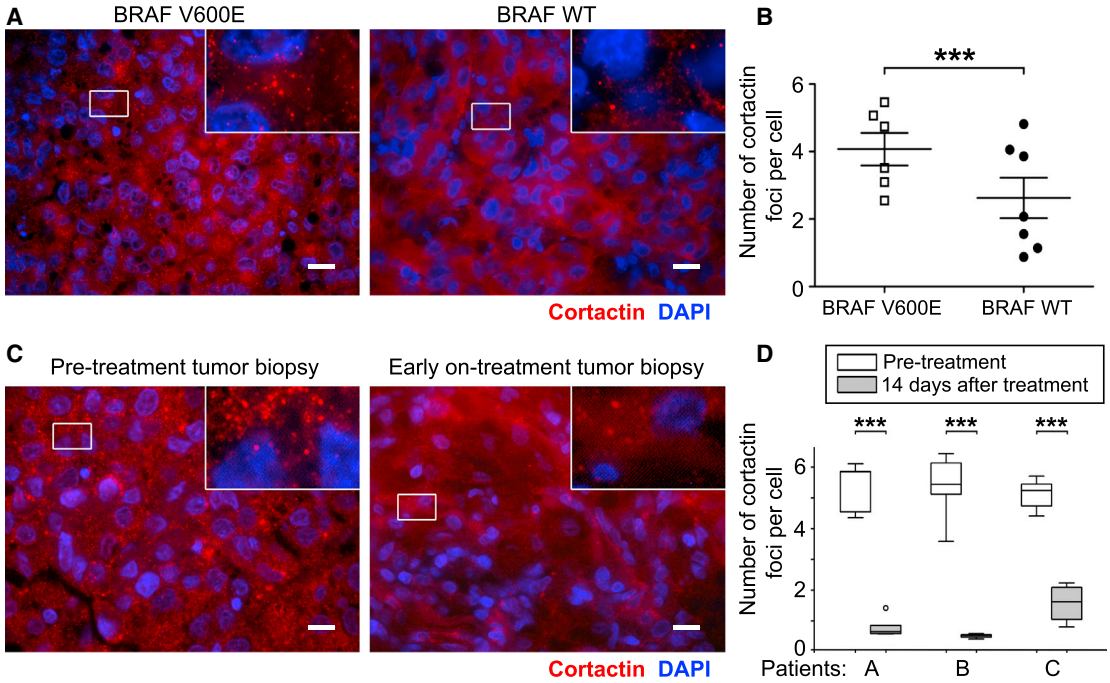

Figure 7. The Number of Cortactin Foci in BRAF^{V600E} Melanoma Patients Decrease upon Vemurafenib Treatment

(A) Representative images of human melanoma samples with wild-type BRAF or human melanoma samples with *BRAF*^{V600E} mutant stained for cortactin (red) and DAPI (blue).

(B) Quantification of cortactin foci in human melanoma samples. n = 6; six field pictures were taken for each melanoma sample.

(C) Representative images of human melanoma samples before treatment or samples after 14 days of vemurafenib treatment.

(D) Quantification of cortactin foci in patient melanoma samples. Pictures of five fields were taken for each melanoma sample.

Scale bars, 50 μm. ***$p < 0.001$. Error bars, SD. Student's t tests were performed using software R v.2.14.

reduced the number of invasive activities, whereas transient expression of *BRAF*^{V600E} promoted cell invasion. Activation of ERK by *BRAF*^{V600E} stimulated the phosphorylation of cortactin and Exo70, which in turn promoted actin reorganization and MMP exocytosis. We further demonstrate that Exo70 knockdown inhibits melanomas metastasis in nude mice. Both pharmacological and genetic extinction of BRAF reduced cortactin foci in the iBIP mouse model. In BRAF-mutated melanoma patients' tumor biopsies, the number of cortactin foci was significantly higher than that in patients with wild-type BRAF; the number of cortactin foci was significantly decreased in patients who received short-term vemurafenib therapy. All of our in vitro and in vivo studies indicate an intimate link between oncogenic BRAF and cell invasion. It was reported that the frequency of BRAF mutation in primary melanomas is comparable to that of metastatic melanomas (Colombino et al., 2012). However, it was also observed that BRAF mutation is associated with a worse outcome at a later tumor stage; the median survival rate of patients with BRAF mutant metastatic melanoma is lower than that of patients with BRAF wild-type melanoma (Long et al., 2011; Menzies et al., 2012). The role of BRAF-mediated cell invasion may contribute to these clinical observations.

We find that short-term expression of *BRAF*^{V600E} is sufficient to promote invasion, whereas long-term expression of *BRAF*^{V600E} induces growth arrest, which is reminiscent of the oncogene-induced senescence (OIS) documented previously (Damsky et al., 2015; Dhomen et al., 2009; Michaloglou et al., 2005; Vredeveld et al., 2012; Wajapeyee et al., 2008). Therefore, it is likely that OIS inhibits the cell invasion phenotype shown at the early stage of *BRAF*^{V600E} expression, which explains the lack of invasion observed in some studies. However, BRAF mutation may provide a critical background for rapid progression to metastatic melanoma once another oncogenic mutation, such as loss of PTEN, occurs (Damsky et al., 2011).

It was also shown that BRAF inhibitors promote tumor metastasis in *RAS* mutant or BRAF inhibitor-resistant melanoma cells (Sanchez-Laorden et al., 2014). As the mitogen-activated protein kinase pathway is reactivated in BRAF inhibitor-resistant cells, this study is consistent with our results and supports the role of RAF-MEK-ERK signaling in melanoma metastasis.

In summary, our studies demonstrate a role of *BRAF*^{V600E} in regulating melanoma invasion. Our data warrant further study of metastatic properties of melanoma and suggest that inhibiting invasion may be a therapeutic strategy for preventing melanoma progression.

EXPERIMENTAL PROCEDURES

Cell Culture, Inhibitor Treatment, and Antibodies

Human melanoma cell lines were isolated from lesions defined by clinical and histological criteria. These cells were cultured in RPMI 1640 medium, 5% fetal bovine serum (v/v). Transfection and RNAi experiments are included in the

Supplemental Information. For inhibitor treatment, cells were incubated with 1 μM PLX4720, 1 μM U0126, or 100 nM GSK1120212 for 24 hr before proceeding to the invadopodia assay. Anti-cortactin antibody was purchased from Santa Cruz, anti-TKS5 and anti-MT1-MMP antibody were purchased from Millipore, anti-phospho-cortactin antibody (S^{418}) was a gift from Dr. Scott Weed (Kelley et al., 2010), and all other antibodies were from Cell Signal.

All clinical data and patients' samples were collected following IRB approval of the Hospital of the University of Pennsylvania, and informed consent was obtained from all study participants. All animal studies were conducted in accordance with NIH animal care and use guidelines, and mice were maintained according to the guidelines of the IACUC of the University of Pennsylvania.

In-Gel Zymography

The in-gel zymography assay for MMP-2 activity was performed as described previously (Liu et al., 2009). Briefly, the serum-free conditioned culture media was collected and concentrated. Samples were snap-frozen three times in liquid nitrogen, mixed with loading buffer, and then separated on an 8% polyacrylamide/0.3% gelatin gel. The gel was washed three times in 2.5% Triton X-100 and then incubated in the MMP reaction buffer (50 mM of Tris-HCl [pH 8.0] and 5 mM of $CaCl_2$) for 36 to 72 hr at 37°C. After the reaction, the gel was stained with Coomassie brilliant blue and destained overnight with destaining buffer.

In Situ Zymography

The protocol used to perform in situ zymography was adapted from the Mueller laboratory (Artym et al., 2009). In brief, Alexa Fluor 568-conjugated gelatin was prepared by Alexa Fluor 568 protein labeling (Molecular Probes). Coverslips were acid-washed and incubated with 50 μg/ml of poly-L-lysine (Sigma) for 20 min and then cross-linked with 0.5% glutaraldehyde (Ted Pella) for 15 min. The coverslips were then inverted onto an 80 μl drop of gelatin (0.2% gelatin and Alexa Fluor 568-labeled gelatin at an 7:1 ratio) for 10 min. After washing in PBS, the coverslips were quenched with 5 mg/ml of $NaBH_4$ for 15 min, followed by another wash with PBS. The coverslips were then incubated in the growth medium; after 2 hr, 2×10^4 cells were plated on the coverslips and incubated at 37°C for 8 hr. The cells were then fixed and stained for immunofluorescence. Each experiment was repeated three times. Gelatin degradation was quantified using ImageJ software.

Immunofluorescence Microscopy

For immunofluorescence assay, cells were fixed with 4% paraformaldehyde/PBS for 15 min and then permeabilized in PBS containing 0.2% Triton X-100 for 5 min. The cells were pre-incubated in 5% BSA/PBS for 30 min and then sequentially incubated with primary and secondary antibodies. Alexa-phalloidin (Molecular Probes) was used for F-actin staining. The images were captured using a Leica CTR6000 confocal microscope at 630× magnification. For tumor tissue immunofluorescence assay, paraffin sections of tumor samples were dewaxed and rehydrated in xylene and graded alcohols. After blocking in 10% BSA/PBST (PBS with 0.5% Tween 20), the samples were incubated with primary antibody overnight at 4°C and then incubated with the second antibody for 2 hr. Finally, the slides were stained in DAPI and mounted with Slowfade mounting buffer. Cells were imaged with the Leica DM IRB microscope at 630× magnification.

Xenograft Tumor Model and iBIP Mouse Model

Xenografts were generated as described previously (Lu et al., 2013). Tumors were palpable at approximately 1 week, and caliper measurements were obtained two times per week. Mice were sacrificed after 5 weeks, and all internal organs were harvested and embedded in paraffin, sectioned, stained with H&E, and then imaged. Mice with cancer metastases were counted, and statistical analysis was performed using Fisher's exact test.

Generation and tumor genesis of iBIP mice was described previously (Kwong et al., 2015). The procedure is included in the Supplemental Information.

Statistical Analysis

Data were analyzed for normality using the Shapiro-Wilk normality test. Nonparametric data were analyzed with Kruskal-Wallis one-way ANOVA, followed by Dunn's multiple comparison test. Data with a normal distribution were analyzed by Student's test. All statistical analyses were performed using software R v.2.14.

Microarray analysis used pre-ranked GSEA. Briefly, all genes were ranked by the Spearman correlation to the length of Dox withdrawal to prioritize genes with monotonic changes over time. The data were then run against the c5 gene ontology gene set, including two additional gene sets, an ERK downregulated gene set previously published (Kwong et al., 2015), and a newly generated and knowledge-based invadopodia gene set.

SUPPLEMENTAL INFORMATION

Supplemental Information includes Supplemental Experimental Procedures and six figures and can be found with this article online at http://dx.doi.org/10.1016/j.celrep.2016.04.073.

AUTHOR CONTRIBUTIONS

H.L., W.G., and X.X. conceived the project and designed and interpreted experiments. S.L., G.Z., Y.Z., L.N.K., J.F., L.W., J.P.M., and M.H. participated in the design and interpretation of mice experiments. H.L., S.L., Y.Z., W.Z., and J.Z. performed the in vitro experiments. Y.H. assisted with statistical analyses. C.K., K.S., M.X., W.X., G.C.K., L.M.S., and P.J.Z. provided melanoma specimens or associated clinical data. H.L. and W.G. wrote the manuscript.

ACKNOWLEDGMENTS

We are grateful to Dr. Scott A. Weed (West Virginia University) for antibodies and Yemin Lan (Drexel University) for assistance in statistical analyses. This work is supported by NIH grant GM085146 to W.G.; NIH grants CA114046, CA25874, and CA174523 to X.X.; and grants CA025874, CA114046, and CA174523 to M.H. M.H. has received research funding from the Dr. Miriam and Sheldon G. Adelson Medical Research Foundation.

Received: November 15, 2015
Revised: January 21, 2016
Accepted: April 19, 2016
Published: May 19, 2016

REFERENCES

Arozarena, I., Sanchez-Laorden, B., Packer, L., Hidalgo-Carcedo, C., Hayward, R., Viros, A., Sahai, E., and Marais, R. (2011). Oncogenic BRAF induces melanoma cell invasion by downregulating the cGMP-specific phosphodiesterase PDE5A. Cancer Cell *19*, 45–57.

Artym, V.V., Yamada, K.M., and Mueller, S.C. (2009). ECM degradation assays for analyzing local cell invasion. Methods Mol. Biol. *522*, 211–219.

Ayala, I., Baldassarre, M., Giacchetti, G., Caldieri, G., Tetè, S., Luini, A., and Buccione, R. (2008). Multiple regulatory inputs converge on cortactin to control invadopodia biogenesis and extracellular matrix degradation. J. Cell Sci. *121*, 369–378.

Bowden, E.T., Barth, M., Thomas, D., Glazer, R.I., and Mueller, S.C. (1999). An invasion-related complex of cortactin, paxillin and PKCmu associates with invadopodia at sites of extracellular matrix degradation. Oncogene *18*, 4440–4449.

Bravo-Cordero, J.J., Hodgson, L., and Condeelis, J. (2012). Directed cell invasion and migration during metastasis. Curr. Opin. Cell Biol. *24*, 277–283.

Carlino, M.S., Haydu, L.E., Kakavand, H., Menzies, A.M., Hamilton, A.L., Yu, B., Ng, C.C., Cooper, W.A., Thompson, J.F., Kefford, R.F., et al. (2014). Correlation of BRAF and NRAS mutation status with outcome, site of distant metastasis and response to chemotherapy in metastatic melanoma. Br. J. Cancer *111*, 292–299.

Casula, M., Colombino, M., Satta, M.P., Cossu, A., Ascierto, P.A., Bianchi-Scarrà, G., Castiglia, D., Budroni, M., Rozzo, C., Manca, A., et al.; Italian Melanoma Intergroup Study (2004). BRAF gene is somatically mutated but does

not make a major contribution to malignant melanoma susceptibility: the Italian Melanoma Intergroup Study. J. Clin. Oncol. *22*, 286–292.

Cho, N.Y., Choi, M., Kim, B.H., Cho, Y.M., Moon, K.C., and Kang, G.H. (2006). BRAF and KRAS mutations in prostatic adenocarcinoma. Int. J. Cancer *119*, 1858–1862.

Colombino, M., Capone, M., Lissia, A., Cossu, A., Rubino, C., De Giorgi, V., Massi, D., Fonsatti, E., Staibano, S., Nappi, O., et al. (2012). BRAF/NRAS mutation frequencies among primary tumors and metastases in patients with melanoma. J. Clin. Oncol. *30*, 2522–2529.

Damsky, W.E., Curley, D.P., Santhanakrishnan, M., Rosenbaum, L.E., Platt, J.T., Gould Rothberg, B.E., Taketo, M.M., Dankort, D., Rimm, D.L., McMahon, M., and Bosenberg, M. (2011). β-catenin signaling controls metastasis in Braf-activated Pten-deficient melanomas. Cancer Cell *20*, 741–754.

Damsky, W., Micevic, G., Meeth, K., Muthusamy, V., Curley, D.P., Santhanakrishnan, M., Erdelyi, I., Platt, J.T., Huang, L., Theodosakis, N., et al. (2015). mTORC1 activation blocks BrafV600E-induced growth arrest but is insufficient for melanoma formation. Cancer Cell *27*, 41–56.

Dankort, D., Curley, D.P., Cartlidge, R.A., Nelson, B., Karnezis, A.N., Damsky, W.E., Jr., You, M.J., DePinho, R.A., McMahon, M., and Bosenberg, M. (2009). Braf(V600E) cooperates with Pten loss to induce metastatic melanoma. Nat. Genet. *41*, 544–552.

Davies, H., Bignell, G.R., Cox, C., Stephens, P., Edkins, S., Clegg, S., Teague, J., Woffendin, H., Garnett, M.J., Bottomley, W., et al. (2002). Mutations of the BRAF gene in human cancer. Nature *417*, 949–954.

Dhomen, N., Reis-Filho, J.S., da Rocha Dias, S., Hayward, R., Savage, K., Delmas, V., Larue, L., Pritchard, C., and Marais, R. (2009). Oncogenic Braf induces melanocyte senescence and melanoma in mice. Cancer Cell *15*, 294–303.

Eckert, M.A., Lwin, T.M., Chang, A.T., Kim, J., Danis, E., Ohno-Machado, L., and Yang, J. (2011). Twist1-induced invadopodia formation promotes tumor metastasis. Cancer Cell *19*, 372–386.

Erdmann, F., Lortet-Tieulent, J., Schüz, J., Zeeb, H., Greinert, R., Breitbart, E.W., and Bray, F. (2013). International trends in the incidence of malignant melanoma 1953–2008—are recent generations at higher or lower risk? Int. J. Cancer *132*, 385–400.

Friedl, P., and Wolf, K. (2003). Tumour-cell invasion and migration: diversity and escape mechanisms. Nat. Rev. Cancer *3*, 362–374.

He, B., and Guo, W. (2009). The exocyst complex in polarized exocytosis. Curr. Opin. Cell Biol. *21*, 537–542.

Hoshino, D., Branch, K.M., and Weaver, A.M. (2013a). Signaling inputs to invadopodia and podosomes. J. Cell Sci. *126*, 2979–2989.

Hoshino, D., Kirkbride, K.C., Costello, K., Clark, E.S., Sinha, S., Grega-Larson, N., Tyska, M.J., and Weaver, A.M. (2013b). Exosome secretion is enhanced by invadopodia and drives invasive behavior. Cell Rep. *5*, 1159–1168.

Hsu, S.C., TerBush, D., Abraham, M., and Guo, W. (2004). The exocyst complex in polarized exocytosis. Int. Rev. Cytol. *233*, 243–265.

Kelley, L.C., Hayes, K.E., Ammer, A.G., Martin, K.H., and Weed, S.A. (2010). Cortactin phosphorylated by ERK1/2 localizes to sites of dynamic actin regulation and is required for carcinoma lamellipodia persistence. PLoS ONE *5*, e13847.

Klein, R.M., Spofford, L.S., Abel, E.V., Ortiz, A., and Aplin, A.E. (2008). B-RAF regulation of Rnd3 participates in actin cytoskeletal and focal adhesion organization. Mol. Biol. Cell *19*, 498–508.

Kwong, L.N., Boland, G.M., Frederick, D.T., Helms, T.L., Akid, A.T., Miller, J.P., Jiang, S., Cooper, Z.A., Song, X., Seth, S., et al. (2015). Co-clinical assessment identifies patterns of BRAF inhibitor resistance in melanoma. J. Clin. Invest. *125*, 1459–1470.

Leong, H.S., Robertson, A.E., Stoletov, K., Leith, S.J., Chin, C.A., Chien, A.E., Hague, M.N., Ablack, A., Carmine-Simmen, K., McPherson, V.A., et al. (2014). Invadopodia are required for cancer cell extravasation and are a therapeutic target for metastasis. Cell Rep. *8*, 1558–1570.

Linder, S. (2007). The matrix corroded: podosomes and invadopodia in extracellular matrix degradation. Trends Cell Biol. *17*, 107–117.

Liu, J.L., Zhu, Q.F., and Hao, B.S. (2008). [Effect of the sera of rabbits fed with Tongxinluo on MMP-9 and TIMP-1 expression and secretion in U937 monocyte-derived macrophages]. Nan Fang Yi Ke Da Xue Xue Bao *28*, 1703–1706.

Liu, J., Yue, P., Artym, V.V., Mueller, S.C., and Guo, W. (2009). The role of the exocyst in matrix metalloproteinase secretion and actin dynamics during tumor cell invadopodia formation. Mol. Biol. Cell *20*, 3763–3771.

Long, G.V., Menzies, A.M., Nagrial, A.M., Haydu, L.E., Hamilton, A.L., Mann, G.J., Hughes, T.M., Thompson, J.F., Scolyer, R.A., and Kefford, R.F. (2011). Prognostic and clinicopathologic associations of oncogenic BRAF in metastatic melanoma. J. Clin. Oncol. *29*, 1239–1246.

Lu, H., Liu, J., Liu, S., Zeng, J., Ding, D., Carstens, R.P., Cong, Y., Xu, X., and Guo, W. (2013). Exo70 isoform switching upon epithelial-mesenchymal transition mediates cancer cell invasion. Dev. Cell *27*, 560–573.

Makrodouli, E., Oikonomou, E., Koc, M., Andera, L., Sasazuki, T., Shirasawa, S., and Pintzas, A. (2011). BRAF and RAS oncogenes regulate Rho GTPase pathways to mediate migration and invasion properties in human colon cancer cells: a comparative study. Mol. Cancer *10*, 118.

Martinez-Quiles, N., Ho, H.Y., Kirschner, M.W., Ramesh, N., and Geha, R.S. (2004). Erk/Src phosphorylation of cortactin acts as a switch on-switch off mechanism that controls its ability to activate N-WASP. Mol. Cell. Biol. *24*, 5269–5280.

McNiven, M.A. (2013). Breaking away: matrix remodeling from the leading edge. Trends Cell Biol. *23*, 16–21.

Meerbrey, K.L., Hu, G., Kessler, J.D., Roarty, K., Li, M.Z., Fang, J.E., Herschkowitz, J.I., Burrows, A.E., Ciccia, A., Sun, T., et al. (2011). The pINDUCER lentiviral toolkit for inducible RNA interference in vitro and in vivo. Proc. Natl. Acad. Sci. USA *108*, 3665–3670.

Menzies, A.M., Haydu, L.E., Visintin, L., Carlino, M.S., Howle, J.R., Thompson, J.F., Kefford, R.F., Scolyer, R.A., and Long, G.V. (2012). Distinguishing clinicopathologic features of patients with V600E and V600K BRAF-mutant metastatic melanoma. Clin. Cancer Res. *18*, 3242–3249.

Michaloglou, C., Vredeveld, L.C., Soengas, M.S., Denoyelle, C., Kuilman, T., van der Horst, C.M., Majoor, D.M., Shay, J.W., Mooi, W.J., and Peeper, D.S. (2005). BRAFE600-associated senescence-like cell cycle arrest of human naevi. Nature *436*, 720–724.

Monteiro, P., Rossé, C., Castro-Castro, A., Irondelle, M., Lagoutte, E., Paul-Gilloteaux, P., Desnos, C., Formstecher, E., Darchen, F., Perrais, D., et al. (2013). Endosomal WASH and exocyst complexes control exocytosis of MT1-MMP at invadopodia. J. Cell Biol. *203*, 1063–1079.

Murphy, D.A., and Courtneidge, S.A. (2011). The "ins" and "outs" of podosomes and invadopodia: characteristics, formation and function. Nat. Rev. Mol. Cell Biol. *12*, 413–426.

Nikiforova, M.N., Kimura, E.T., Gandhi, M., Biddinger, P.W., Knauf, J.A., Basolo, F., Zhu, Z., Giannini, R., Salvatore, G., Fusco, A., et al. (2003). BRAF mutations in thyroid tumors are restricted to papillary carcinomas and anaplastic or poorly differentiated carcinomas arising from papillary carcinomas. J. Clin. Endocrinol. Metab. *88*, 5399–5404.

Nürnberg, A., Kitzing, T., and Grosse, R. (2011). Nucleating actin for invasion. Nat. Rev. Cancer *11*, 177–187.

Paz, H., Pathak, N., and Yang, J. (2014). Invading one step at a time: the role of invadopodia in tumor metastasis. Oncogene *33*, 4193–4202.

Poulikakos, P.I., Persaud, Y., Janakiraman, M., Kong, X., Ng, C., Moriceau, G., Shi, H., Atefi, M., Titz, B., Gabay, M.T., et al. (2011). RAF inhibitor resistance is mediated by dimerization of aberrantly spliced BRAF(V600E). Nature *480*, 387–390.

Ren, J., and Guo, W. (2012). ERK1/2 regulate exocytosis through direct phosphorylation of the exocyst component Exo70. Dev. Cell *22*, 967–978.

Roth, A.D., Tejpar, S., Delorenzi, M., Yan, P., Fiocca, R., Klingbiel, D., Dietrich, D., Biesmans, B., Bodoky, G., Barone, C., et al. (2010). Prognostic role of KRAS and BRAF in stage II and III resected colon cancer: results of the translational study on the PETACC-3, EORTC 40993, SAKK 60-00 trial. J. Clin. Oncol. *28*, 466–474.

Sakurai-Yageta, M., Recchi, C., Le Dez, G., Sibarita, J.B., Daviet, L., Camonis, J., D'Souza-Schorey, C., and Chavrier, P. (2008). The interaction of IQGAP1 with the exocyst complex is required for tumor cell invasion downstream of Cdc42 and RhoA. J. Cell Biol. *181*, 985–998.

Sanchez-Laorden, B., Viros, A., Girotti, M.R., Pedersen, M., Saturno, G., Zambon, A., Niculescu-Duvaz, D., Turajlic, S., Hayes, A., Gore, M., et al. (2014). BRAF inhibitors induce metastasis in RAS mutant or inhibitor-resistant melanoma cells by reactivating MEK and ERK signaling. Sci. Signal. *7*, ra30.

Seals, D.F., Azucena, E.F., Jr., Pass, I., Tesfay, L., Gordon, R., Woodrow, M., Resau, J.H., and Courtneidge, S.A. (2005). The adaptor protein Tks5/Fish is required for podosome formation and function, and for the protease-driven invasion of cancer cells. Cancer Cell *7*, 155–165.

Sharma, V.P., Eddy, R., Entenberg, D., Kai, M., Gertler, F.B., and Condeelis, J. (2013). Tks5 and SHIP2 regulate invadopodium maturation, but not initiation, in breast carcinoma cells. Curr. Biol. *23*, 2079–2089.

Ugurel, S., Thirumaran, R.K., Bloethner, S., Gast, A., Sucker, A., Mueller-Berghaus, J., Rittgen, W., Hemminki, K., Becker, J.C., Kumar, R., and Schadendorf, D. (2007). B-RAF and N-RAS mutations are preserved during short time in vitro propagation and differentially impact prognosis. PLoS ONE *2*, e236.

Van Cutsem, E., Köhne, C.H., Láng, I., Folprecht, G., Nowacki, M.P., Cascinu, S., Shchepotin, I., Maurel, J., Cunningham, D., Tejpar, S., et al. (2011). Cetuximab plus irinotecan, fluorouracil, and leucovorin as first-line treatment for metastatic colorectal cancer: updated analysis of overall survival according to tumor KRAS and BRAF mutation status. J. Clin. Oncol. *29*, 2011–2019.

Vredeveld, L.C., Possik, P.A., Smit, M.A., Meissl, K., Michaloglou, C., Horlings, H.M., Ajouaou, A., Kortman, P.C., Dankort, D., McMahon, M., et al. (2012). Abrogation of BRAFV600E-induced senescence by PI3K pathway activation contributes to melanomagenesis. Genes Dev. *26*, 1055–1069.

Wajapeyee, N., Serra, R.W., Zhu, X., Mahalingam, M., and Green, M.R. (2008). Oncogenic BRAF induces senescence and apoptosis through pathways mediated by the secreted protein IGFBP7. Cell *132*, 363–374.

Wan, P.T., Garnett, M.J., Roe, S.M., Lee, S., Niculescu-Duvaz, D., Good, V.M., Jones, C.M., Marshall, C.J., Springer, C.J., Barford, D., and Marais, R.; Cancer Genome Project (2004). Mechanism of activation of the RAF-ERK signaling pathway by oncogenic mutations of B-RAF. Cell *116*, 855–867.

Wu, B., and Guo, W. (2015). The exocyst at a glance. J. Cell Sci. *128*, 2957–2964.

Yamaguchi, H. (2012). Pathological roles of invadopodia in cancer invasion and metastasis. Eur. J. Cell Biol. *91*, 902–907.

Yokota, T., Ura, T., Shibata, N., Takahari, D., Shitara, K., Nomura, M., Kondo, C., Mizota, A., Utsunomiya, S., Muro, K., and Yatabe, Y. (2011). BRAF mutation is a powerful prognostic factor in advanced and recurrent colorectal cancer. Br. J. Cancer *104*, 856–862.